

Electronic state around vortex in a two-band superconductor

Masanori Ichioka* and Kazushige Machida

Department of Physics, Okayama University, Okayama 700-8530, Japan

Noriyuki Nakai

Yukawa Institute for Theoretical Physics, Kyoto University, Kyoto 606-8502, Japan

Predrag Miranović

Department of Physics, University of Montenegro, Podgorica 81000, Serbia and Montenegro

(Dated: November 14, 2018)

Based on the quasiclassical theory, we investigate the vortex state in a two-band superconductor with a small gap on a three dimensional Fermi surface and a large gap on a quasi-two dimensional one, as in MgB₂. The field dependence of zero-energy density of states is compared for fields parallel and perpendicular to the *ab* plane, and the anisotropy of the vortex core shape is discussed for a parallel field. The Fermi surface geometry of two-bands, combining the effect of the normal-like electronic state on the small gap band at high fields, produces characteristic behavior in the anisotropy of *c*- and *ab*-directions.

PACS numbers: 74.25.Op, 74.25.Qt, 74.25.Jb, 74.70.Ad

I. INTRODUCTION

Since there are many materials with a multi-band structure, it is important to study the contribution of the multi-band structure on superconductivity in order to understand the superconducting state in these materials.¹ Superconductivity of MgB₂ has been well studied both experimentally and theoretically after its discovery.² Now it is recognized that MgB₂ is a typical example of a multi-band superconductor, which has two bands and two superconducting gaps, i.e., a large superconducting gap in the σ band and a small gap in the π band.^{3,4,5,6,7}

On the other hand, the electronic states around the vortex when applying a magnetic field can be a probe for the anisotropy of the superconducting gap and the Fermi surface structure. The field dependence of the density of states (DOS) $N(E=0)$ depends on the gap anisotropy.^{8,9} From the field orientation dependence of $N(E=0)$ we can obtain information of the node position in anisotropic superconductors.¹⁰ These features are examined experimentally by the specific heat or thermal conductivity measurements.^{11,12}

When this analysis is applied to MgB₂, we detect the feature of two-band and Fermi surface anisotropy. The rapid increase in the field dependence of the DOS at low fields as $N(E=0) \sim H^0$ ²³ and the large vortex core size observed by scanning tunneling microscopy (STM) in MgB₂ are understood as characteristics of two-band superconductivity.^{13,14,15} These come from the contribution of the small gap band, whose electronic state becomes normal-like state by applying a weak magnetic field, as explained by theoretical calculations for $H \parallel c$.^{16,17,18} Therefore, characters of a two-band superconductor are understood for $H \parallel c$.

As the next step, two-band characters are examined for $H \parallel ab$, or by field-orientation dependence. In the

field-orientation dependence, the contributions from the isotropic three dimensional (3D) Fermi surface as shown in Fig. 1(a) are expected to be isotropic. On the other hand, the quasi-two dimensional (Q2D) Fermi surface as shown in Fig. 1(b) gives an anisotropic contribution, reflecting the coherence length ratio ξ_{ab}/ξ_c , which is related to the Fermi velocity anisotropy ratio $(|v_{ab}|^2)^{1/2}/(|v_c|^2)^{1/2}$. As the contributions of the σ -band with a Q2D Fermi surface and a π -band with a 3D Fermi surface are coupled in MgB₂ and the dominant contribution changes depending on the field range, the study for $H \parallel ab$ or for field-orientation dependence is important in order to further extract the information of a two-band superconductor and the Fermi surface anisotropy.

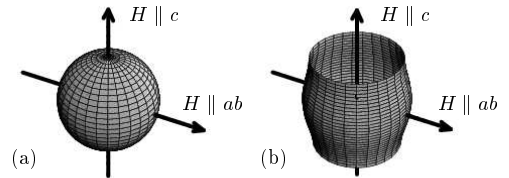


FIG. 1: Schematic view of the isotropic 3D Fermi surface (a) and Q2D Fermi surface (b). We consider the cases of two magnetic field orientations, $H \parallel c$ and $H \parallel ab$.

Focusing on this point, some experimental studies and analyses were performed. In the specific heat and the thermal conductivity measurement,^{19,20} the field-dependences are compared for $H \parallel ab$ and $H \parallel c$, which shows that only a slight difference between $N(E=0, H \parallel c)$ and $N(E=0, H \parallel ab)$ is observed at low fields, while at high fields there is a pronounced anisotropy. This result was explained due to the fact that the dominant

isotropic contribution to $N(E=0)$ at low fields is coming from the π band with a 3D Fermi surface, and high field anisotropic behaviors are due to the σ band with a Q2D Fermi surface. The different temperature dependence of anisotropy ratios $\gamma_H = H_{c2,ab}/H_{c2,c}$ and $\gamma_\lambda = \lambda_c/\lambda_{ab}$ is also a consequence of this multi-gap (multi-band) nature of superconductivity in MgB₂.²¹ There were some works studying the contribution of 3D and Q2D Fermi surface sheets on the vortex state by quasiclassical theory.^{18,22,23} There, H_{c2} -behavior is compared for $H \parallel c$ and $H \parallel ab$, and the electronic states of the vortex state were discussed for $H \parallel c$. In this study, we discuss the electronic state of the vortex states mainly for $H \parallel ab$.

For $H \parallel ab$, it is important to examine the vortex core shape, since the core shape is determined by the anisotropy ratio of the coherence length. For this purpose, we selfconsistently determine the profile of the order parameter in the vortex state. In this field-orientation $H \parallel ab$, we expect a highly anisotropic core shape from the Q2D Fermi surface contribution of the σ band. However, the vortex core image for $H \parallel ab$ observed by STM shows that the vortex core is a circular shape at a low field.²⁴ This indicates that the anisotropic contribution of a Q2D Fermi surface is not clear and that the contribution of the 3D Fermi surface is dominant in the vortex core image of STM at this field range.

The purpose of this paper is to investigate the electronic state of the vortex lattice state mainly for $H \parallel ab$ using quasiclassical theory in the clean limit of a two-band superconductor with 3D and Q2D Fermi surfaces. The quasiclassical theory can be applied in all range of temperatures and magnetic fields. After describing our formulation of the quasiclassical theory in Sec. II, we analyze the field dependence of $N(E=0)$ comparing two field orientations $H \parallel ab$ and $H \parallel c$ in Sec. III, and clarify the contributions of multi-gap superconductivity and the Fermi surface geometries. In Sec. IV, we study the vortex core structure and the local density of states (LDOS), which are observed by STM, and discuss the anisotropy of the vortex core shape for $H \parallel ab$. In Sec. V, we show the quasiparticle excitation spectrum outside vortex core to see the behavior of the gap edge at finite fields. The last section is devoted to summary and discussions.

II. FORMULATION

We consider a simplified model of a two-band system with a large superconducting gap band and a small gap band (denoted as L-band and S-band, respectively). For simplicity, the superconducting gap at each band is assumed isotropic. We use the following model of the 3D and Q2D Fermi surfaces.^{18,22,23} As shown in Fig. 1(a), the S-band corresponding to the π -band is assumed to have a spherical Fermi surface, given by $E_S(\mathbf{k}_F) = (\hbar^2/2m)(k_{Fx}^2 + k_{Fy}^2 + k_{Fz}^2) = E_F$ with Fermi energy $E_F = \hbar^2 k_F^2/2m$. Fermi velocity is given by $\mathbf{v}(\mathbf{k}_{FS}) = \partial E_S/\partial \mathbf{k} = v_{F0}(k_x, k_y, k_z)/k_F =$

$v_{F0}(\sin \theta \cos \phi, \sin \theta \sin \phi, \cos \theta)$ with $0 \leq \theta < \pi$ and $0 \leq \phi < 2\pi$. As shown in Fig. 1(b), the L-band is assumed to have a Q2D Fermi surface of cylinder-like shape with small ripples, given by $E_L(\mathbf{k}_F) = (\hbar^2/2m)(k_x^2 + k_y^2) - t \cos k_z = E_F$ and Fermi velocity $\mathbf{v}(\mathbf{k}_{FL}) = v_{F0L}(\cos \phi, \sin \phi, \tilde{v}_z \sin k_z)$, where \tilde{v}_z is small and related to the anisotropy ratio as $1/\tilde{v}_z \sim \gamma_H$. In our calculation, we set $1/\tilde{v}_z = 6$ and $v_{FL0} = v_{F0}$.

Vortex structure and electronic states are calculated by quasiclassical Eilenberger theory in the clean limit.^{9,25,26,27} First, the quasiclassical Green's functions $g(i\omega_n, \mathbf{k}_{Fj}, \mathbf{r})$, $f(i\omega_n, \mathbf{k}_{Fj}, \mathbf{r})$ and $f^\dagger(i\omega_n, \mathbf{k}_{Fj}, \mathbf{r})$ are calculated in a unit cell of the vortex lattice by solving Eilenberger equation

$$\{\omega_n + \tilde{\mathbf{v}}(\mathbf{k}_{Fj}) \cdot [\nabla + i\mathbf{A}(\mathbf{r})]\} f = \Delta_j(\mathbf{r})g, \quad (1)$$

$$\{\omega_n - \tilde{\mathbf{v}}(\mathbf{k}_{Fj}) \cdot [\nabla - i\mathbf{A}(\mathbf{r})]\} f^\dagger = \Delta_j^*(\mathbf{r})g \quad (2)$$

in the so-called explosion method, where $g = (1 - f f^\dagger)^{1/2}$, $\text{Reg} > 0$, $\tilde{\mathbf{v}}(\mathbf{k}_{Fj}) = \mathbf{v}(\mathbf{k}_{Fj})/v_{F0}$, $j = L, S$, and Matsubara frequency $\omega_n = (2n + 1)\pi T$. In the symmetric gauge, $\mathbf{A}(\mathbf{r}) = \frac{1}{2}\mathbf{B} \times \mathbf{r} + \mathbf{a}(\mathbf{r})$, where $\mathbf{B} = (0, 0, B)$ is a uniform field and $\mathbf{a}(\mathbf{r})$ is related to the internal field $\mathbf{b}(\mathbf{r})$ as $\mathbf{b}(\mathbf{r}) = \nabla \times \mathbf{a}(\mathbf{r})$. The unit vectors of the vortex lattice are given by $\mathbf{u}_1 = (a_x, 0, 0)$, and $\mathbf{u}_2 = (\frac{1}{2}a_x, a_y, 0)$. The pair potential and vector potential are selfconsistently calculated by the relations

$$\Delta_j(\mathbf{r}) = 2T \sum_{\omega_n > 0} \sum_{j', \mathbf{k}_{Fj'}} V_{jj'} f(i\omega_n, \mathbf{k}_{Fj'}, \mathbf{r}), \quad (3)$$

$$\mathbf{J}(\mathbf{r}) = -2T \tilde{\kappa}^{-2} \sum_{\omega_n > 0} \sum_{j, \mathbf{k}_{Fj}} \mathbf{v}(\mathbf{k}_{Fj}) \text{Im}g(i\omega_n, \mathbf{k}_{Fj}, \mathbf{r}), \quad (4)$$

where $\mathbf{J}(\mathbf{r}) = \nabla \times \nabla \times \mathbf{A}(\mathbf{r})$, and $\tilde{\kappa} = (7\zeta(3)/18)^{1/2} \kappa_{\text{BCS}}$ with Riemann's zeta function $\zeta(3)$. We set the energy cut-off $\omega_c = 20T_{c0}$, $\kappa_{\text{BCS}} = 30$, and the DOS in normal state at each Fermi surface $N_{0L} = N_{0S} = 0.5N_0$. The integral $\sum_{j, \mathbf{k}_{Fj}}$ takes account of N_{0j} and the \mathbf{k}_F -dependent DOS ($\propto |\mathbf{v}(\mathbf{k}_{Fj})|^{-1}$) on the Fermi surface. The LDOS is given by

$$\begin{aligned} N_{\text{total}}(E, \mathbf{r}) &= \sum_{j=L,S} N_j(E, \mathbf{r}) \\ &= \sum_{j, \mathbf{k}_{Fj}} \text{Reg}(i\omega_n \rightarrow E + i\eta, \mathbf{k}_{Fj}, \mathbf{r}), \end{aligned} \quad (5)$$

where g is obtained by solving Eqs. (1) and (2) under $i\omega_n \rightarrow E + i\eta$. We typically use $\eta = 0.01$. The spatial average of the LDOS gives DOS;

$$N_{\text{total}}(E) = \sum_{j=L,S} N_j(E) = \langle N(E, \mathbf{r}) \rangle_{\mathbf{r}}. \quad (6)$$

We assume that superconductivity in the S-band occurs by Cooper pair transfer V_{LS} from the L-band. Therefore, we set the pairing interaction $V_{SS} = 0$ in the S-band, and use $V_{SL} = 0.32V_{LL}$ so that $\Delta_L/\Delta_S \sim 3$ at

a zero field. Throughout this paper, temperatures, energies, lengths, magnetic fields, and DOS are, respectively, measured in units of T_{c0} , $\pi k_B T_{c0}$, $R_0 = \hbar v_{F0}/2\pi k_B T_{c0}$, $B_0 = \phi_0/2\pi R_0^2$ and N_0 , where T_{c0} is the superconducting transition temperature in the case $V_{LS} = V_{SS} = 0$. Our calculation is performed at $T = 0.1T_{c0}$. The shape of the vortex lattice for $H \parallel c$ is the triangular lattice with $a_x/(2a_y/\sqrt{3}) = 1$. For $H \parallel ab$, the anisotropic ratio $a_x/(2a_y/\sqrt{3})$ of the vortex lattice varies from 1.2 at low fields to $\gamma_H \sim 6$ at high fields in MgB_2 .^{24,28} We study two cases $a_x/(2a_y/\sqrt{3}) = 1.5$ and 6 for this field orientation.

We selfconsistently calculate the order parameter $\Delta_L(\mathbf{r})$, $\Delta_S(\mathbf{r})$ and the vector potential $\mathbf{a}(\mathbf{r})$, under a given vortex lattice ratio $a_x/(2a_y/\sqrt{3})$. We alternatively solve the Eilenberger equations [Eqs. (1) and (2)] and the self-consistent condition [Eqs. (3) and (4)], until a sufficiently selfconsistent solution is obtained. As an initial state of the calculation, we use the Abrikosov solution of the lowest Landau level for $\Delta_L(\mathbf{r})$, and set $\Delta_S(\mathbf{r}) = 0$ and $\mathbf{a}(\mathbf{r}) = 0$. By this selfconsistent calculation, we can properly estimate the size and shape of the vortex core. In the Abrikosov solution, vortex core size is always proportional to the inter-vortex distance. In our selfconsistent method, the vortex core size remains to be in the order of the coherence length even when the inter-vortex distance becomes large at low fields. This proper treatment of the vortex core size is necessary to correctly estimate the low energy excitations of the quasiparticles especially at low fields. The selfconsistently obtained $\mathbf{a}(\mathbf{r})$ does not give a significant contribution on the electronic state, since we consider the case of high- κ .

III. FIELD DEPENDENCE OF ZERO-ENERGY DENSITY OF STATES

At low fields, low energy quasiparticles are localized around vortex cores in full-gap superconductors. With increasing field, the distribution of low energy quasiparticles around a vortex core overlaps with that coming from neighbor vortex cores, since inter-vortex distance decreases.²⁷ Therefore, low energy quasiparticles extend outside of the vortex core. The zero-energy total DOS $N_{\text{total}}(E = 0)$ is the spatial average of these low-energy quasiparticle distributions. Field dependence of total DOS $N_{\text{total}}(E = 0)$ and each band contribution $N_L(E = 0)$ and $N_S(E = 0)$ are shown in Fig. 2(a) both for $H \parallel ab$ and $H \parallel c$. The DOS on the S-band increases rapidly at low fields, and saturates to normal state value $0.5N_0$ at higher fields. The increase of total DOS at high fields is due to the L-band contribution. These are consistent with previous calculations.^{16,17,18}

In this study, we compare the curves for $H \parallel ab$ and $H \parallel c$. The rapidly increasing S band contribution N_S is almost the same for both orientations at low fields, reflecting the 3D isotropic Fermi surface shape. Slowly increasing the L-band contribution N_L shows a large difference, reflecting the anisotropy of H_{c2} dominantly com-

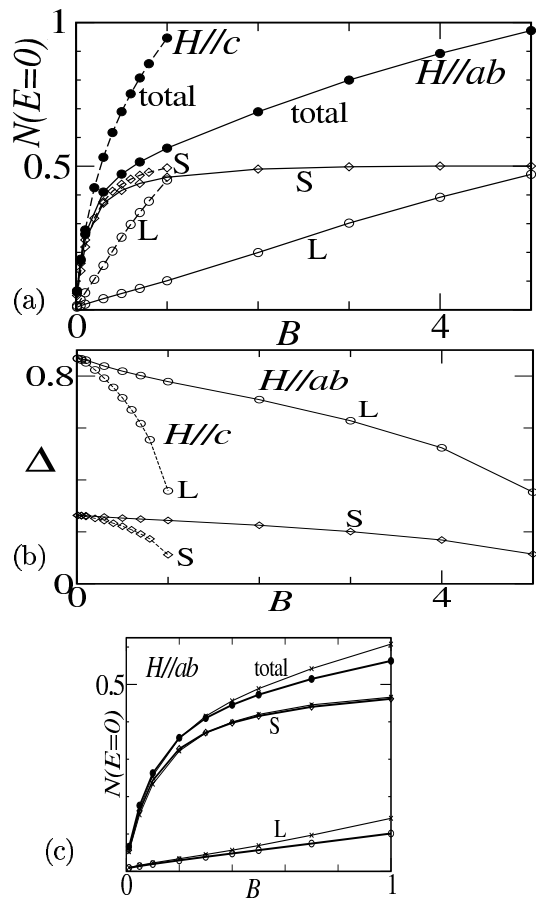


FIG. 2: (a) Field dependence of zero-energy DOS $N_{\text{total}} = N_L + N_S$ (\bullet) for $H \parallel ab$ (solid lines) and $H \parallel c$ (dashed lines). Large-gap band contributions N_L (\circ) and small-gap band contributions N_S (\diamond) are also presented. Vortex lattice ratio $a_x/(2a_y/\sqrt{3}) = 6$ for $H \parallel ab$ and 1 for $H \parallel c$. (b) Field dependence of maximum pair potential amplitudes $|\Delta_L|$ (\circ) and $|\Delta_S|$ (\diamond) in the vortex lattice state for $H \parallel ab$ (solid lines) and $H \parallel c$ (dashed lines). (c) Field dependence of zero-energy DOS for $a_x/(2a_y/\sqrt{3}) = 1.5$ (thin lines with \times) and 6 (thick lines) for $H \parallel ab$ at low fields.

ing from the Q2D Fermi surface. As a result, N_{total} is almost isotropic at low fields, and largely anisotropic at higher fields, which is consistent with experimental observations.^{19,20}

Figure 2(b) indicates that, while electronic states in the S-band are normal-like state at high fields, the pair potential Δ_S in the S-band persists up to H_{c2} with a gap ratio $|\Delta_L|/|\Delta_S|$ relatively unchanged, as well as that Δ_S persists up to T_c at $H = 0$.^{4,5,6} This is easy to understand since superconductivity in the S-band is induced by the Cooper pair transfer from the L-band. As long as we have the pair potential $|\Delta_L|$ in the L-band, the induced pair potential in S-band is non-vanishing. This behavior is similar both for $H \parallel c$ and $H \parallel ab$.

It is necessary to see how DOS depends on the anisotropic ratio $a_x/(2a_y/\sqrt{3})$ for a unit cell of the vortex lattice, which is given in our calculation. We plot the

DOS for $a_x/(2a_y/\sqrt{3})=6$ and 1.5 in Fig. 2(c). At low fields, DOS does not significantly depend on the shape of the unit cell, because low-energy electrons are localized around vortex cores. Therefore, our numerical results do not significantly depend on the delicate tuning of the vortex lattice ratio $a_x/(2a_y/\sqrt{3})$ at low fields. At higher fields, where the low-energy quasiparticles around vortices overlap each other, there appears a deviation depending on the vortex lattice shape. At these fields, however, the equilibrium vortex lattice in MgB₂ is a distorted hexagonal with $a_x/(2a_y/\sqrt{3}) \sim \gamma_H \sim 6$.²⁸ Therefore, it is reasonable to study the vortex structure with $a_x/(2a_y/\sqrt{3}) = 6$ at high fields.

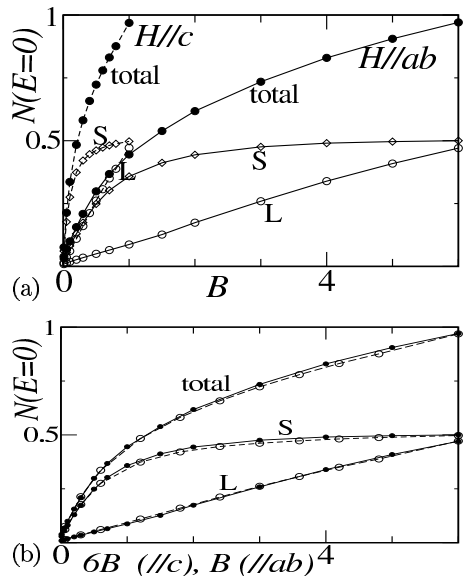


FIG. 3: (a) Field dependence of DOS N_{total} (\bullet), N_L (\circ) and N_S (\diamond) for $H \parallel ab$ (solid lines) and $H \parallel c$ (dashed lines) when both bands have Q2D Fermi surfaces with $1/\tilde{v}_z = 6$. $a_x/(2a_y/\sqrt{3}) = 6$. (b) Field dependence of (a) is replotted as a function of $6B$ for $H \parallel c$ (B for $H \parallel ab$), as $\gamma_H \sim 6$.

To show an example that the field-dependence of N_{total} is changed by the Fermi surface geometry in a two-band superconductor, we also calculate the case when both L- and S-bands have Q2D cylindrical Fermi surfaces with $1/\tilde{v}_z = 6$, for comparison. In this case, as shown in Fig. 3(a), field-dependences of N_{total} are anisotropic between $H \parallel ab$ and $H \parallel c$ both at low and high field, because S-band contributions at low fields are also anisotropic due to the Q2D Fermi surface contribution. When all bands have the same Fermi surface geometry as in this case, we can expect that H -dependences of $N_{\text{total}}(E=0)$ are roughly scaled by H_{c2} anisotropy. In Fig. 3(b), the field dependences of zero-energy DOS are replotted as a function of $6B$ for $H \parallel c$ (B for $H \parallel ab$) as $\gamma_H \sim 6$. There, calculated data of N_{total} (and also N_L , N_S) for $H \parallel ab$ and $H \parallel c$ are on the same curve, i.e., field dependences are well scaled by H_{c2} anisotropy. On the other hand, the field dependences in Fig. 2(a) are not scaled by the H_{c2} ratio, because the two bands have different geometry,

i.e., 3D and Q2D Fermi surfaces.

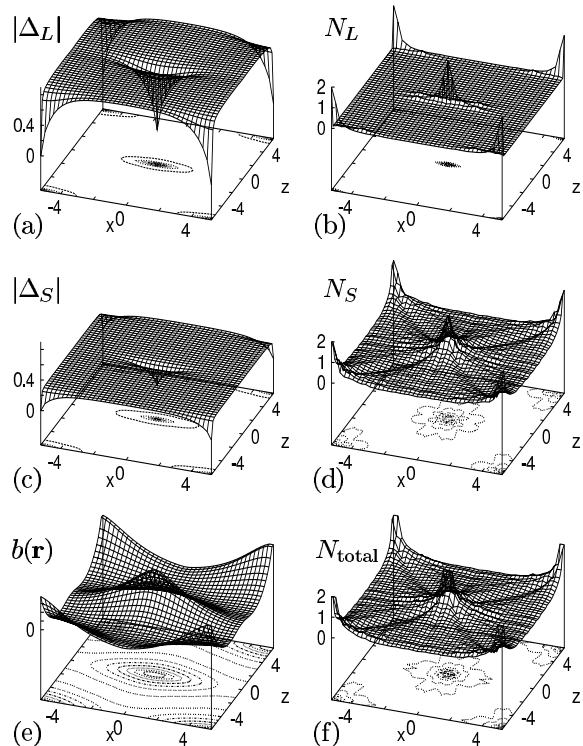


FIG. 4: Spatial structure of vortex lattice state for $H \parallel ab$. $B = 0.1$ and $a_x/(2a_y/\sqrt{3}) = 1.5$. The vortex centers are located in the middle and at the four corners of the figure. The pair potential amplitude $|\Delta_L(\mathbf{r})|$ (a) and $|\Delta_S(\mathbf{r})|$ (c). Internal field $b(\mathbf{r})$ (e). Zero-energy LDOS $N_{\text{total}}(E=0, \mathbf{r})$ (f) and each band contribution $N_L(E=0, \mathbf{r})$ (b) and $N_S(E=0, \mathbf{r})$ (d). The peaks are truncated at $N = 2N_0$.

IV. VORTEX CORE STRUCTURE FOR PARALLEL FIELDS

We study the vortex core structure and the LDOS around the vortex for $H \parallel ab$ in order to see how the anisotropy of the vortex core shape is affected by 3D or Q2D Fermi surfaces. Figure 4 shows the vortex structure for $H \parallel ab$ at $B = 0.1$. In this low field case, we use the vortex lattice ratio $a_x/(2a_y/\sqrt{3}) = 1.5$ for the unit cell of the vortex lattice. Looking at the amplitude of the selfconsistently calculated pair potential $|\Delta_L(\mathbf{r})|$ [(a)] and $|\Delta_S(\mathbf{r})|$ [(c)] under the given vortex lattice ratio, one can notice that the vortex core shape is highly anisotropic due to the effect of the Q2D Fermi surface. The anisotropy of internal field $b(\mathbf{r})$ [(e)] is not so large. The LDOS on the L-band, $N_L(E=0, \mathbf{r})$ [(b)], is highly anisotropic, reflecting anisotropy of $|\Delta_L(\mathbf{r})|$. However, the LDOS on S-band, $N_S(E=0, \mathbf{r})$ [(d)], shows isotropic distribution reflecting 3D Fermi surface. The LDOS around the vortex core is broad on the S-band, as in the case $H \parallel c$.^{15,16,17} Since the S-band contribution

is dominant at this low field, as discussed in Fig. 2(a), the total LDOS $N_{\text{total}}(E = 0, \mathbf{r})$ [(f)] shows the isotropic vortex core shape, reflecting $N_S(E = 0, \mathbf{r})$. This corresponds to an almost isotropic vortex core shape observed by STM.²⁴ The highly anisotropic L-band contribution is masked by the S-band contribution. Therefore, while the pair potential around the vortex core is highly anisotropic reflecting the Q2D Fermi surface, the dominant contribution of the S-band with the 3D Fermi surface gives an isotropic vortex core image in the quasiparticle excitations observed by STM.

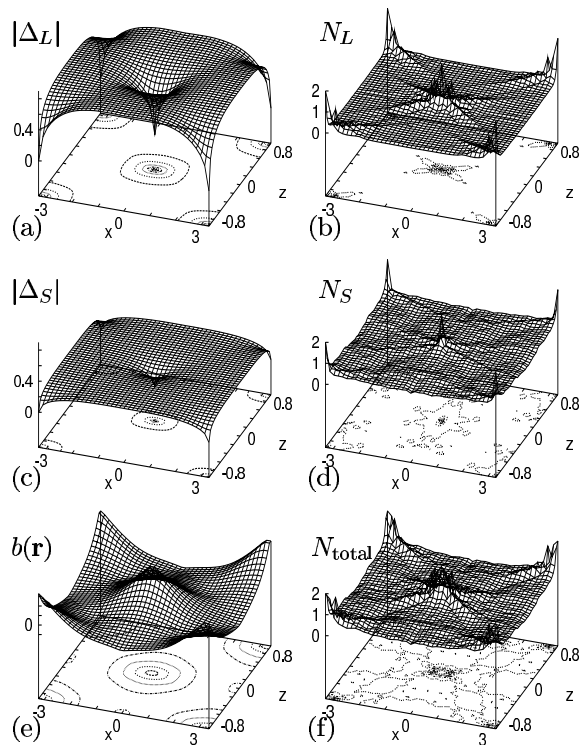


FIG. 5: The same as Fig. 4, but $B = 1$ and $a_x/(2a_y/\sqrt{3}) = 6$. It is noted that scales of x and z are anisotropic in this figure of a highly distorted hexagonal vortex lattice case at high fields.

Figure 5 shows the vortex structure at a higher field $B = 1$, where we use the vortex lattice ratio of a highly distorted hexagonal, $a_x/(2a_y/\sqrt{3}) = 6$. The difference of overall views in Figs. 4 and 5 also comes from the deformation of the vortex lattice. While the vortex core structures of $|\Delta_L(\mathbf{r})|$ [(a)], $|\Delta_S(\mathbf{r})|$ [(c)] and $N_L(E = 0, \mathbf{r})$ [(b)] are similar to those in Fig. 4, they are seen as if they are isotropic in this figure scaled by the coherence length ratio $\gamma_H \sim 6$. That is, when we see the pair potential amplitude and $N_L(E = 0, \mathbf{r})$, the vortex core structure is highly anisotropic, reflecting the Q2D Fermi surface, both at low and high fields. The anisotropy around the vortex in $b(\mathbf{r})$ increases with raising the field, and saturates to that of γ_H as is seen in Fig. 5(e). By the effect of increasing the field, $N_S(E = 0, \mathbf{r})$ [(d)] is almost flat and slightly enhanced at the vortex center. Therefore, the

vortex core shape in the total LDOS $N_{\text{total}}(E = 0, \mathbf{r})$ [(f)] reflects the spatial structure of $N_L(E = 0, \mathbf{r})$ at higher fields.

V. LOCAL SPECTRUM FAR FROM VORTEX CORE

As mentioned above, while both pair potentials $|\Delta_L|$ and $|\Delta_S|$ survive up to H_{c2} , the electronic state in the S-band becomes a normal-like state at high fields. The field range of this normal-like state is wider for $H \parallel ab$. Therefore, it is interesting to see how the superconducting gap edges at $|\Delta_L|$ and $|\Delta_S|$ in the quasiparticle excitation spectrum are smeared by the quasiparticle excitations in the vortex states.

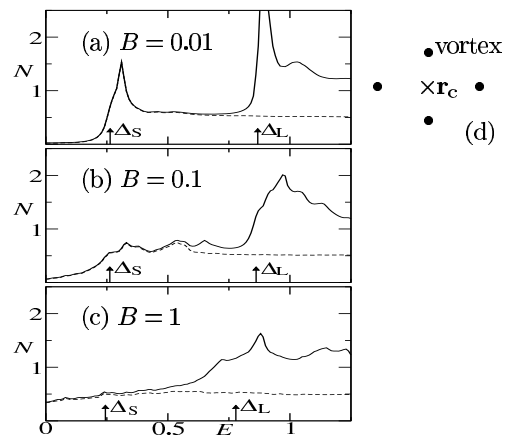


FIG. 6: Local spectrum $N_{\text{total}}(E, \mathbf{r}_c)$ [solid lines] and the S-band contribution $N_S(E, \mathbf{r}_c)$ [dashed lines] for $H \parallel ab$ at the midpoint \mathbf{r}_c of the surrounding four vortices as shown in (d). $B = 0.01$ (a), 0.1 (b) and 1 (c). $a_x/(2a_y/\sqrt{3}) = 1.5$ ($B = 0.01, 0.1$) and 6 ($B = 1$). Arrows in the figure indicate $|\Delta_L|$ and $|\Delta_S|$ at each field, presented in Fig. 2(b).

The local spectrum $N_{\text{total}}(E, \mathbf{r}_c)$ is shown in Fig. 6 at the point \mathbf{r}_c far from vortex cores, where the superconducting gap structure in the spectrum may survive up to higher fields, compared with other points. At a low field $B = 0.01$ [Fig. 6(a)], S-band and L-band contributions, respectively, have clear gap edges at $E \sim \Delta_S$ and Δ_L . With increasing B [Fig. 6(b)], low energy DOS extending from the vortex core grows up within the gap edge, and the gap edge is smeared. The smearing is eminent for the lower excitation gap of Δ_S , whose excitation gap structure comes from the S-band contribution $N_S(E, \mathbf{r}_c)$. At high field $B = 1$ [Fig. 6(c)], $N_S(E, \mathbf{r}_c)$ is almost flat, i.e., normal-like state. While there are some attempts to observe the field dependence of Δ_S by STM,^{29,30} the excitation gap of Δ_S becomes difficult to be observed at the field range of a normal-like state S-band state.

VI. SUMMARY AND DISCUSSIONS

Based on the quasiclassical theory, the electronic structure in the vortex state was studied in a two-band superconductor with the 3D and Q2D Fermi surfaces, mainly for $H \parallel ab$. To demonstrate the appearance of the effect due to the geometry of the 3D and Q2D Fermi surfaces, we compared the field dependence of zero-energy DOS for $H \parallel ab$ and $H \parallel c$, and analyzed the anisotropy of the vortex core structure for $H \parallel ab$. The 3D and Q2D Fermi surfaces, respectively, introduce the isotropic and anisotropic contribution, when c - and ab - orientations are compared. At low (high) fields, dominant contribution to the change of the total DOS is coming from the small (large) gap band which has the isotropic 3D (anisotropic Q2D) Fermi surface. Therefore, the field-dependence of zero-energy DOS shows isotropic (anisotropic) behavior, when the field-orientation is changed. This reproduces the results of specific heat and thermal conductivity measurements.^{19,20} As for the vortex core anisotropy, the pair potential around the vortex core is highly anisotropic reflecting the Q2D Fermi surface. However, the dominant contribution of the low-energy quasiparticle state, coming from the S-band with a 3D Fermi surface, gives an isotropic vortex core image at low fields. This may be a

explanation of the almost circular vortex core image by STM in MgB₂ even when $H \parallel ab$.²⁴

As is seen in DOS, LDOS and spectrum, the electronic state on the S-band is normal-like state in a wide field range at higher fields. However, this does not mean that the pair potential $|\Delta_S|$ on the S-band vanishes in this field region. Quite contrary, $|\Delta_S|$ persists up to H_{c2} since superconductivity in the S-band is induced by the Cooper pair transfer from the L-band. The origin of a normal-like electronic state on the S-band is the contribution of low energy excitations by a supercurrent around vortex cores, coupling with the vortex core state of the quasiparticles. With an increasing magnetic field, the low energy excitations are enhanced, and those low energy quasiparticles around the vortex are delocalized giving rise to large LDOS between vortices. For the small gap in the S-band, the low field gives enough excitations to smear the gap structure of Δ_S , resulting in a normal-like electronic state. We demonstrated that MgB₂ shows characteristic behavior in the anisotropy of c - and ab -axis directions, by coupling of the effect of these normal-like electronic states in the S-band at high fields and the effect of the Fermi surface geometry (3D and Q2D Fermi surfaces) in a two-band superconductor.

-
- * Electronic address: oka@mp.okayama-u.ac.jp
- ¹ H. Suhl, B.T. Matthias, and L.R. Walker, Phys. Rev. Lett. **3**, 552 (1959).
 - ² J. Nagamatsu, N. Nakaga, T. Muranaka, Y. Zenitani, and J. Akimitsu, Nature (London) **410**, 63 (2001).
 - ³ J. Kortus, I.I. Mazin, K.D. Belashchenko, V.P. Antropov, and L.L. Boyer, Phys. Rev. Lett. **86**, 4656 (2001).
 - ⁴ R.S. Gonnelli, D. Daghero, G.A. Ummarino, V.A. Stepanov, J. Jun, S.M. Kazakov, and J. Karpinski, Phys. Rev. Lett. **89**, 247004 (2002).
 - ⁵ M. Iavarone, G. Karapetrov, A.E. Koshelev, W.K. Kwok, G.W. Crabtree, D.G. Hinks, W.N. Kang, E-M. Choi, H.J. Kim, H-J. Kim, and S.I. Lee, Phys. Rev. Lett. **89**, 187002 (2002).
 - ⁶ S. Tsuda, T. Yokoya, T. Kiss, Y. Takano, K. Togano, H. Kito, H. Ihara, and S. Shin, Phys. Rev. Lett. **87**, 177006 (2001).
 - ⁷ S. Souma, Y. Machida, T. Sato, T. Takahashi, H. Matsui, S.-C. Wang, H. Ding, A. Kaminski, J. C. Campuzano, S. Sasaki, and K. Kadowaki, Nature (London) **423**, 65 (2003).
 - ⁸ G.E. Volovik, JETP Lett. **58**, 469 (1993).
 - ⁹ M. Ichioka, A. Hasegawa, and K. Machida, Phys. Rev. B **59**, 184 (1999); **59**, 8902 (1999).
 - ¹⁰ P. Miranović, N. Nakai, M. Ichioka, and K. Machida, Phys. Rev. B **68**, 052501 (2003).
 - ¹¹ T. Park, M.B. Salamon, E.M. Choi, H.J. Kim, and S.I. Lee, Phys. Rev. Lett. **90**, 177001 (2003).
 - ¹² K. Izawa, K. Kamata, Y. Nakajima, Y. Matsuda, T. Watanabe, M. Nohara, H. Takagi, P. Thalmeier, and K. Maki, Phys. Rev. Lett. **89**, 137006 (2002).
 - ¹³ H.D. Yang, J.-Y. Lin, H.H. Li, F.H. Hsu, C.J. Liu, S.-C. Li, R.-C. Yu, and C.-Q. Jin, Phys. Rev. Lett. **87**, 167003 (2001).
 - ¹⁴ F. Bouquet, R.A. Fisher, N.E. Phillips, D.G. Hinks, and J.D. Jorgensen, Phys. Rev. Lett. **87**, 047001 (2001).
 - ¹⁵ M.R. Eskildsen, M. Kugler, S. Tanaka, J. Jun, S.M. Kazakov, J. Karpinski, and Ø. Fischer, Phys. Rev. Lett. **89**, 187003 (2002).
 - ¹⁶ N. Nakai, M. Ichioka, and K. Machida, J. Phys. Soc. Jpn. **71**, 23 (2002).
 - ¹⁷ A.E. Koshelev and A.A. Golubov, Phys. Rev. Lett. **90**, 177002 (2003).
 - ¹⁸ T. Dahm, S. Graser, and N. Schopohl, Physica C **408-410**, 336 (2004).
 - ¹⁹ F. Bouquet, Y. Wang, I. Sheikin, T. Plackowski, A. Junod, S. Lee, and S. Tajima, Phys. Rev. Lett. **89**, 257001 (2002).
 - ²⁰ A. Shibata, M. Matsumoto, K. Izawa, and Y. Matsuda, S. Lee, and S. Tajima, Phys. Rev. B **68**, 060501 (2003).
 - ²¹ P. Miranović, K. Machida, and V.G. Kogan, J. Phys. Soc. Jpn. **72**, 221 (2003).
 - ²² T. Dahm and N. Schopohl, Phys. Rev. Lett. **91**, 017001 (2003).
 - ²³ S. Graser, T. Dahm, and N. Schopohl, Phys. Rev. B **69**, 014511 (2004).
 - ²⁴ M.R. Eskildsen, N. Jenkins, G. Levy, M. Kugler, Ø. Fischer, J. Jun, S.M. Kazakov, and J. Karpinski, Phys. Rev. B **68**, 100508 (2003).
 - ²⁵ G. Eilenberger, Z. Phys. **214**, 195 (1968).
 - ²⁶ U. Klein, J. Low Temp. Phys. **69**, 1 (1987).
 - ²⁷ M. Ichioka, N. Hayashi, and K. Machida, Phys. Rev. B **55**, 6565 (1997).
 - ²⁸ R. Cubitt, M.R. Eskildsen, C.D. Dewhurst, J. Jun, S.M. Kazakov, and J. Karpinski, Phys. Rev. Lett. **91**, 047002 (2003).

- ²⁹ Y. Bugoslavsky, Y. Miyoshi, G.K. Perkins, A.D. Caplin, L.F. Cohen, A.V. Pogrebnyakov, and X.X. Xi, Phys. Rev. B **69**, 132508 (2004).
- ³⁰ R.S. Gonnelli, D. Daghero, A. Calzolari, G.A. Ummarino,

V. Dellarocca, V.A. Stepanov, J. Jun, S.M. Kazakov, and J. Karpinski, Phys. Rev. B **69**, 100504 (2004).